



High-temperature tensile strength of near-stoichiometric SiC/SiC composites

K. Hironaka^{a,*}, T. Nozawa^a, T. Hinoki^a, N. Igawa^b, Y. Katoh^{a,c},
L.L. Snead^d, A. Kohyama^{a,c}

^a Institute of Advanced Energy, Kyoto University, Gokasho, Uji, Kyoto 611-0011, Japan

^b Japan Atomic Energy Research Institute, Tokai, Ibaraki 319-1195, Japan

^c CREST-ACE, Japan Science and Technology Corporation, 4-1-8 Honcho, Kawaguchi, Saitama 332-0012, Japan

^d Oak Ridge National Laboratory, P.O. Box 2008, Oak Ridge, TN 37830-6087, USA

Abstract

In an attempt to characterize mechanical properties of near-stoichiometric SiC/SiC composites, tensile tests were conducted at room temperature in air and at elevated temperature under mild oxidizing gases atmosphere. SiC/SiC composites were fabricated by forced-flow chemical vapor infiltration method using two-dimensional fabrics of carbon coated near-stoichiometric Tyranno™SA fibers. Tensile tests were conducted on composites with two types of lay-up schemes using edge-loading small specimens. The effect of lay-up orientation on the mechanical properties and fracture behavior of composites were also examined. Tensile strength of composite was slightly decreased at 1573 K, while it retained approximately 80% of the strength at room temperature. Porosity dependence on elastic modulus was clearly exhibited.

© 2002 Published by Elsevier Science B.V.

1. Introduction

SiC/SiC composites are one of the promising materials for fusion energy applications because of their excellent high-temperature mechanical properties and low activation properties under severe radiation environments [1–3]. The improvement of more thermally stable and radiation-resistant SiC/SiC composites could be achieved by near-stoichiometric fiber and matrix. Advanced SiC fibers, such as Hi-Nicalon™type-S and Tyranno™SA, are chemically and structurally similar to stoichiometric SiC with lower oxygen contents, comparing with early generation SiC fibers. Forced-flow/thermal-gradient chemical vapor infiltration technique (FCVI) was developed at Oak Ridge National Laboratory (ORNL), which can produce a fully crystalline and

stoichiometric SiC matrix with shorter times compared with conventional isothermal [4,5].

As a part of the US–Japan collaboration project, fabrication techniques of large scale SiC/SiC composites with near-stoichiometric fibers by FCVI process are now being developed. These composites are expected to have excellent high temperature properties owing to near-stoichiometric composition. This study focused on tensile properties of SiC/SiC composites with advanced near-stoichiometry SiC fibers for the optimization of FCVI process.

For the evaluation of mechanical properties of ceramic matrix composites after neutron irradiation, small specimen test technique has been developed [6–8]. Instead of flexure tests, tensile tests technique using small specimen was introduced as more reliable method to evaluate mechanical performance [9]. This technique is also useful for the evaluation of high temperature strength.

The objective of this work is to evaluate tensile properties of near-stoichiometric SiC/SiC composites at room temperature and at high temperature in mild

* Corresponding author. Tel.: +81-774 38 3463; fax: +81-774 38 3467.

E-mail address: keisuke@iae.kyoto-u.ac.jp (K. Hironaka).

oxidizing environment. Tensile tests were conducted to the composites using edge-loading small specimens. Dependence of porosity and carbon layer thickness on mechanical properties was also examined.

2. Experimental

2.1. Materials

Plane-woven fabrics of Tyranno™ SA fiber (Ube Industries) were used for performance with a fabric layer orientation of $[-30^\circ/0^\circ/30^\circ]$ and $[0^\circ/90^\circ]$. As fiber/matrix interface, pyrolytic carbon layers of different thickness were deposited on fibers. The fiber preforms were placed in the FCVI furnace, and then infiltrated with methyltrichlorosilane (MTS) carried by hydrogen. The material properties for fabricated disks were summarized in Table 1.

2.2. Mechanical property testing

Tensile test specimens were cut out from the fabricated disks with 7.6 cm diameters and 1.7 cm thickness. The schematic illustration of tensile specimen used in this work was shown in Fig. 1. Total length of specimen was determined by the inner size of irradiation capsule, about 50 mm or less. While, gauge length was about 15–20 mm in order to leave enough gripping area and to make it easy to compare with our previous result about specimen size effects [6,7]. The slop of specimen edge shoulder was determined following ASTM Standard C1275. The gauge thickness was 2.3 mm due to the obtained material limitation. Transition between gauge section and edge section was naturally curved in order to reduce stress concentration and this radius was determined by finite element method analysis. The specimens were loaded at their shoulder edge by SiC fixture. Tensile tests were conducted by an electromechanical testing machine (Instron Japan Co., Ltd.). All tests were conducted at a rate of 0.5 mm/min in crosshead speed. The step-loading tensile tests were performed for room-

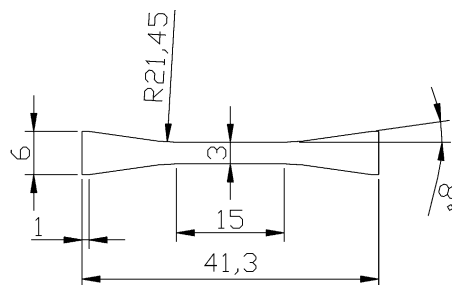


Fig. 1. Edge-loaded small tensile specimen (dimension: mm).

temperature tension in air for the precise evaluation of damage accumulation near proportional limit. Monotonic tensile tests were conducted for high-temperature tension at 1573 K in a flow of commercial argon, in which the oxygen partial pressure was estimated to be approximately 0.1 Pa. The test fixture and specimen were heated at a rate of 20 K/min to the test temperature and were allowed to equilibrate for 5–10 min before starting tensile test. After the fracture, the specimens were examined by using scanning electron microscopy. Besides, porosity and thickness of PyC interphase near fracture plane was also measured.

3. Results and discussion

Fig. 2 shows representative tensile stress–strain curves for $[-30^\circ/0^\circ/30^\circ]$ and $[0^\circ/90^\circ]$ composites tested at room temperature. Up to proportional limit stress (PLS), these two curves exhibited similar behavior while following nonlinear behaviors were quite different. The large reduction of the slope for hysteresis in $[-30^\circ/0^\circ/30^\circ]$ SiC/SiC was shown. Also $[-30^\circ/0^\circ/30^\circ]$ SiC/SiC had larger accumulation of strain. These indicated more damage was accumulated in $[-30^\circ/0^\circ/30^\circ]$ SiC/SiC. In Fig. 3, tensile properties at RT were shown. Here, the PLS was the stress corresponding to 0.005% offset strain. Composites exhibited high elastic modulus owing to crystalline matrix and fiber. In spite of the difference of

Table 1
Material properties of FCVI–SiC/SiC composites

Fabric information		PW fabrication of interphase		PyC material properties		
Sample ID	Orientation	Nominal thickness (nm)	Measured average thickness (nm)	Estimated fiber volume fraction (vol.%)	Estimated density (mg/m ³)	Measured porosity (%)
1256	$[-30^\circ/0^\circ/30^\circ]$	150	107.1	37	2.76	15.1
1260	$[-30^\circ/0^\circ/30^\circ]$	300	168.5	30.2	2.28	24.2
1261	$[-30^\circ/0^\circ/30^\circ]$	75	70.5	33.3	2.54	20.4
1264	$[0^\circ/90^\circ]$	150	116.4	35.4	2.61	23.3
1265	$[0^\circ/90^\circ]$	300	225.5	35.3	2.72	18.0
1266	$[0^\circ/90^\circ]$	75	42.3	35.2	2.62	18.1

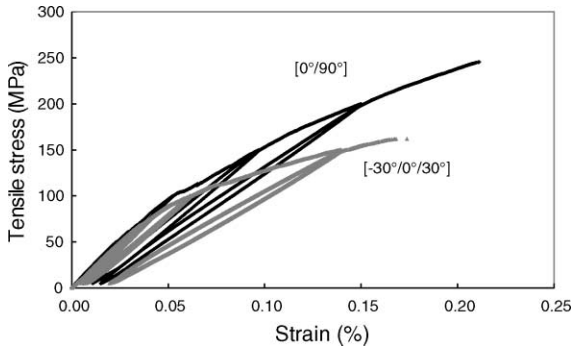


Fig. 2. Stress–strain behavior of SiC/SiC composites at room temperature.

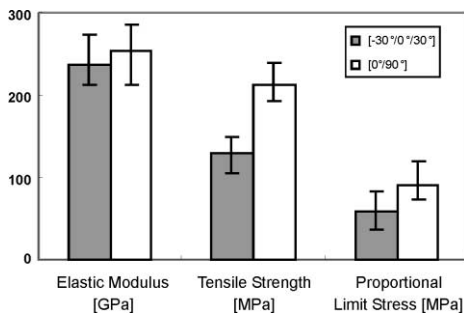


Fig. 3. Tensile properties of $[-30^\circ/0^\circ/30^\circ]$ and $[0^\circ/90^\circ]$ SiC/SiC composites.

fabric orientation, elastic modulus and PLS were almost same. On the contrary, ultimate tensile strength of $[-30^\circ/0^\circ/30^\circ]$ SiC/SiC was approximately 60% of $[0^\circ/90^\circ]$ SiC/SiC. Suppose that fiber strength aligned in the tensile axis made most significant effect on composite strength, then $[0^\circ/90^\circ]$ SiC/SiC, with higher volume fraction of fibers in tensile axis, showed higher tensile strength than $[-30^\circ/0^\circ/30^\circ]$ SiC/SiC.

Porosity dependence on tensile properties was investigated (Fig. 4). Elastic modulus linearly increased with smaller porosity (Fig. 4(a)). This could be explained by the fact that the mixture of the modulus of each component determines tensile modulus. It was revealed that ultimate tensile strength had no clear relationship with porosity (Fig. 4(b)). It is well known that maximum stress significantly depends on axial fiber volume fraction [7,10]. Therefore, tensile strength may not change if the quantity of fibers is constant in each specimen. In flexure, there was a clear relationship between maximum strength and porosity, and flexural strength was nearly proportional to density [11]. This is due to the difference of key fracture mode that works on composite fracture. In tension, delamination, dominant in flexure, would not make a significant effect on fracture behavior at maximum stress.

Fracture surface after tensile tests at RT are shown in Fig. 5(a), (b). Relatively short fiber pull-outs were seen in 0° bundles although any appreciable individual fiber pull-outs could not be seen in bundles oriented in other direction. Bundle fracture was characteristic in $-30^\circ, 30^\circ$ bundles. This means that two different fracture mode, tension and shear, exist in $[-30^\circ/0^\circ/30^\circ]$ composites.

Fig. 6 shows the dependence of carbon coating thickness on tensile strength. It was revealed that tensile strength was nearly independent of carbon coating thickness. In flexure, the existence of optimum carbon coating thickness to achieve maximum strength was reported [11]. However, fracture mode in flexure is combination of tension, compression, interlaminar shear and so on. Therefore, for the discussion of optimum coating thickness, the dependence of each fracture mode needs to be investigated.

Comparison of tensile strength at room and high temperature were shown in Fig. 7. Tensile strength slightly decreased at 1573 K to approximately 80% of the strength at room temperature. Since SiC fiber and matrix used in this study were near-stoichiometric

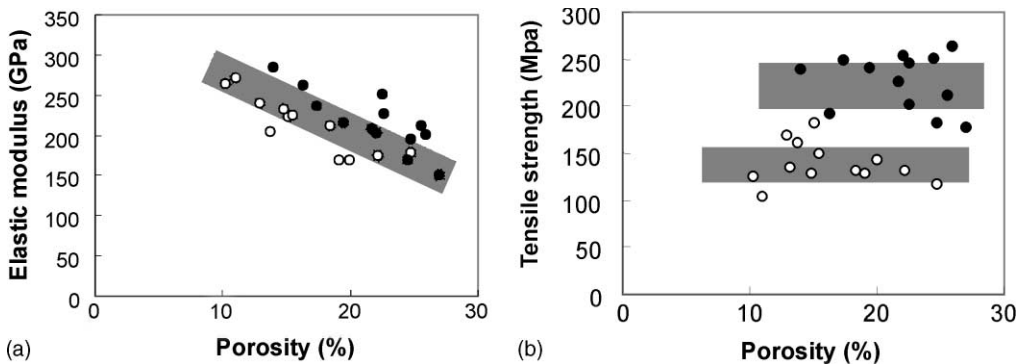


Fig. 4. Porosity dependence on tensile properties: (a) elastic modulus and (b) tensile strength: (● $[0^\circ/90^\circ]$, ○ $[-30^\circ/0^\circ/30^\circ]$).

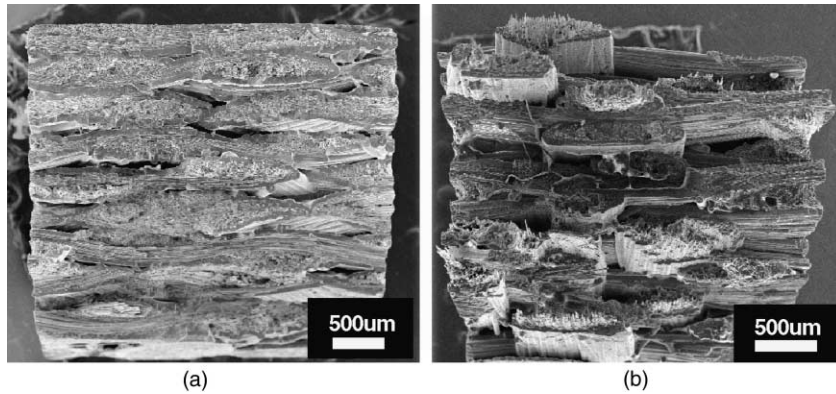


Fig. 5. Fracture surfaces of SiC/SiC composites after tensile test at room temperature: (a) $[-30^\circ/0^\circ/30^\circ]$ (ID:1256) and (b) $[0^\circ/90^\circ]$ (ID:1264).

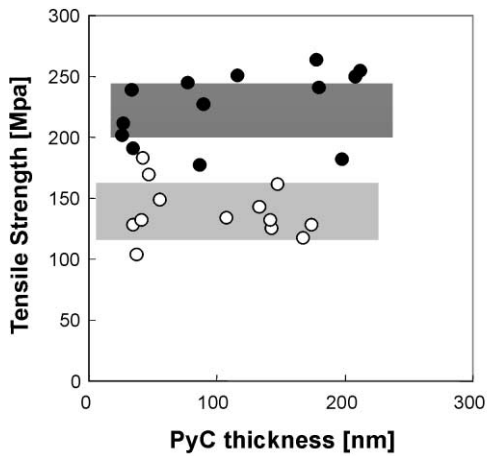


Fig. 6. Dependence of carbon layer thickness on tensile strength: ●: $[0^\circ/90^\circ]$, ○: $[-30^\circ/0^\circ/30^\circ]$.

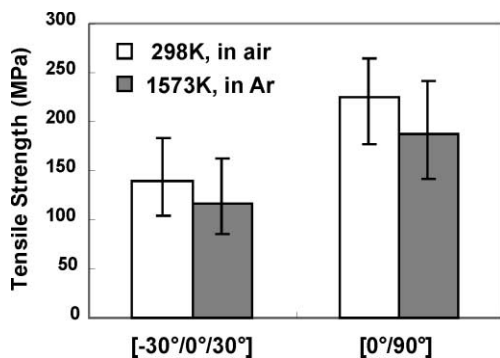


Fig. 7. Comparison of tensile strength at room and high temperature.

composition, there should be no degradation of their strength under test condition. Therefore, PyC interphase

should have some change at HT. Fracture surface after high temperature tensile test was apparently same as that of room temperature, but the loss of carbon coating was observed near the surface of specimen. However, this was only limited to the surface of specimen, it is unlikely that this caused the reduction of tensile strength. The decrease of fiber-matrix interfacial sliding stress might be the reason for the reduction of tensile strength.

4. Conclusion

Mechanical properties of near-stoichiometric SiC/SiC composites fabricated by forced-flow chemical vapor infiltration were evaluated at room and high temperature using edge load small tensile specimen. The following conclusions were derived from Section 3.

Tensile strength was slightly decreased at 1573 K in mild oxidizing environment, while it retained approximately 80% of the strength at room temperature. The decrease of fiber-matrix interfacial sliding stress might be the reason for the reduction of tensile strength. Elastic modulus could be increased by decreasing the porosity. Porosity dependence on tensile strength could not be seen.

Acknowledgements

The authors are grateful to Mr J.C. McLaughlin, Oak Ridge National Laboratory, and Mr T. Taguchi, Japan Atomic Energy Research Institute, for fabricating materials. The materials studied in this work were supplied by the Japan–USA Program of Irradiation Test for Fusion Research (JUPITER).

References

- [1] L.L. Snead, Y. Katoh, A. Kohyama, J.L. Bailey, N.L. Vaughn, R.A. Lowden, *J. Nucl. Mater.* 283–287 (2000) 551.
- [2] L. Giancarli, G. Aiello, A. Gasse, G. Le Marois, Y. Poitevin, J.F. Salavy, J. Szczepanski, *Fus. Eng. Des.* 48 (2000) 509.
- [3] P. Fenici, A.J. Frias Rebelo, R.H. Jones, A. Kohyama, L.L. Snead, *J. Nucl. Mater.* 258–263 (1998) 215.
- [4] T.M. Besmann, J.C. McLaughlin, L. Hua-Tay, *J. Nucl. Mater.* 219 (1995) 31.
- [5] K.J. Probst, T.M. Besmann, D.P. Stinton, R.A. Lowden, T.J. Anderson, T.L. Starr, *Surf. Coat. Technol.* 120&121 (1999) 250.
- [6] T. Nozawa, T. Hinoki, Y. Katoh, A. Kohyama, E. Lara-Curzio, M. Sato, *Adv. Ceram. Compos.* VI 124 (2001) 351.
- [7] T. Nozawa, T. Hinoki, Y. Katoh, A. Kohyama, E. Lara-Curzio, *ASTM STP* 1418, in press.
- [8] A. Kruglov, K. Hironaka, A. Kohyama, M. Bulkanov, Ju. Pevchikh, V. Troyanov, *J. Nucl. Mater.*, in press.
- [9] T. Nozawa, K. Hironaka, Y. Katoh, A. Kohyama, E. Lara-Curzio, *J. Nucl. Mater.*, in press.
- [10] W.A. Curtin, *Compos. Sci. Technol.* 543 (2000) 60.
- [11] W. Yang, H. Araki, T. Noda, J.Y. Park, Y. Katoh, T. Hinoki, J. Yu, A. Kohyama, *J. Am. Ceram. Soc.*, submitted for publication.